

A Solar Radiation Prediction Model Using Weather Forecast Data and Regional Atmospheric Data

Jinsoo Han and Wan-Ki Park

Electronics and Telecommunications Research Institute, Daejeon, 34129, Republic of Korea

Abstract — Photovoltaic generation fluctuates depending on weather conditions. A reliable prediction of it is required for efficient use of it. This paper proposes a solar radiation prediction model using weather forecast and regional atmospheric data. Parameters not in weather forecast data are shown to be calculated from other parameters in the weather data. Simulation is carried out using hourly weather data of one year. The simulation results show that the cross correlation coefficient between the predicted and measured radiations is 0.947 and the model is reliable enough to predict hourly solar radiations.

Index Terms — solar radiation prediction, weather forecast, photovoltaic, hourly radiation.

I. INTRODUCTION

Increasing deployment of photovoltaic (PV) generation system has contributed the expansion of green energy to the future energy supply. The PV generation is proportional to the solar radiation which is affected by weather and the sun's position; thus, the PV power fluctuates. Hence, a reliable prediction of solar energy is required for an efficient use of it.

Several studies have estimated global horizontal radiations based on various radiation models using weather and regional atmospheric data [1]-[4]. The weather data includes temperature, humidity, cloud cover index, air pressure, and so on. The regional atmospheric data includes visibility, ground reflectivity, atmospheric albedo, and so on. The sun's position can be calculated using astronomical equations. Therefore, solar radiation can be estimated based on the weather, the regional atmospheric, and the sun's position data.

This paper proposes a solar radiation prediction model using weather forecast data and regional atmospheric data. The prediction model is verified by simulation and analysis over the measured hourly global horizontal irradiance (GHI) data.

II. SOLAR RADIATION PREDICTION MODEL

A. Direct and Diffuse Irradiance Model

Solar irradiance is composed of two components: direct and diffuse [4]. *Iqbal model C* gives the direct normal irradiance (DNI), I_n , as follows:

$$I_n = 0.9751E_o I_{sc} T_r T_o T_g T_w T_a \quad (\text{W/m}^2). \quad (1)$$

E_o is the eccentricity-correction factor related to the distance between the earth and the sun. I_{sc} is the solar constant, 1367

W/m². T_r , T_o , T_g , T_w , and T_a are Rayleigh, ozone, gas, water-vapor, and aerosol transmittances in the air, respectively. Various weather, atmospheric, and regional parameters affect the five transmittances. Fig. 1 shows the relations between parameters for direct irradiance. The zenith angle, θ_z , is calculated using astronomical equations based on date, time, longitude, and latitude; it affects the air mass, m_r . P and P_0 are actual and standard air pressures, respectively; they affect an actual air mass, m_a . T_r and T_g are affected by m_a . Vis is a visibility; it is affected by an atmospheric turbidity. T_a is affected by m_a and Vis . ϵ_w (cm) is a precipitable water-vapor thickness (PWVT); it affects T_w . ϵ_o (cm) is a vertical ozone thickness; it affects T_o . P and ϵ_w are weather data. Vis and ϵ_o are regional atmospheric data. The five transmittances are expressed as a mathematical form using those parameters as shown in Fig. 1 [3]-[5].

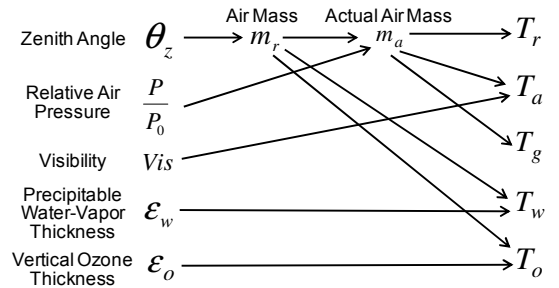


Fig. 1 Relations between various parameters for direct irradiance.

The diffuse horizontal irradiance (DHI), I_d , is classified into three components: 1) Rayleigh scattering, I_{dr} , 2) aerosol scattering, I_{da} , 3) scattering by multiple reflections between the ground and the air, I_{dm} [3]-[6]. The DHI is the sum of three components as follows:

$$I_d = I_{dr} + I_{da} + I_{dm} \quad (\text{W/m}^2). \quad (2)$$

Fig. 2 shows the relations between air transmittances, diffuse irradiance components, and other regional parameters. The three diffuse irradiances are calculated using equations based on the above obtained transmittances such as T_r , T_o , T_w , and T_a ; and the regional atmospheric data such as w_o , r_a , r_g , and B_a [3], [6]. First, I_{dr} and I_{da} are calculated based on the zenith angle and four transmittances. Second, I_{dm} are calculated based on I_{dr} , I_{da} , and other parameters.

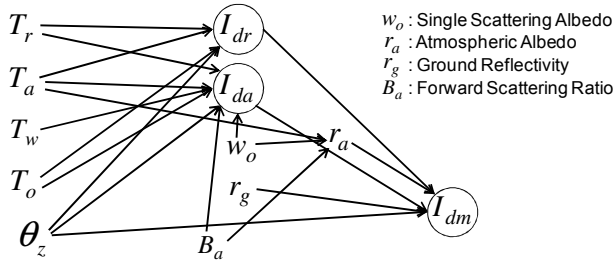


Fig. 2 Relations between various transmittances and regional parameters for diffuse irradiances.

After I_n and I_d are calculated, the global horizontal irradiance (GHI) under clear skies, I_T , is calculated. The zenith angle, θ_z , is considered to calculate the direct horizontal irradiance perpendicular to the surface. The GHI is written as

$$I_T = I_n \cos \theta_z + I_d \text{ (W/m}^2\text{)}. \quad (3)$$

Cloud cover index (CCI) is an important parameter to estimate solar radiations under cloudy skies. It is known that the ratio of global radiation for any given cloud amount to global radiation is independent for solar altitude [7]. The global radiation under cloudy skies, I_{Tc} , is expressed as

$$I_{Tc} = I_T (1 - C(N/K)^D) \text{ (W/m}^2\text{)}. \quad (4)$$

The C and D are the regional coefficients related to the cloud effects; the K is the maximum cloud index; the N shows CCI and ranges from 0 to K. Therefore, the GHI under cloudy skies on a specific time and region can be estimated using equations (1)-(4).

B. Input Parameters Setup for Irradiance Model

The parameters in both weather and regional atmospheric data need to be specified to estimate solar irradiance on a specific time and region. The Vis , ϵ_w , w_o , r_a , r_g , and B_a are regional atmospheric data. Those values are specified in relation to the region. However, generally, weather forecast does not include air pressure, P , and PWVT, ϵ_w . Therefore, a certain method is needed to calculate those two unknown parameters based on the weather forecast data.

First, as in Fig. 1, the air pressure affects the actual air mass, m_a ; the actual air mass affects the three air transmittances, T_r , T_a , and T_g . Hence, the unknown air pressure makes prediction of solar radiation difficult. Although the air pressure varies day by day and hour by hour, it has seasonal variation trend. So, past monthly average air pressure will be considered instead of actual forecasted air pressure. Generally, monthly variation is within a few percent. Fig. 3 shows the combined transmittance variation of T_r , T_a , and T_g over the varying zenith angles and relative air pressures. The larger the zenith angle is, the larger the transmittance error is. The transmittance varies from 1.64% ~ 2.26% over 8% variation of the relative air pressure. In the Republic of Korea, the monthly variation of air pressure

is less than 2.4 %. As a result, the transmittance error caused by air pressure variations is less than 0.7%. Hence, monthly average air pressures from the past weather data can replace air pressures excluded from the weather forecast data.

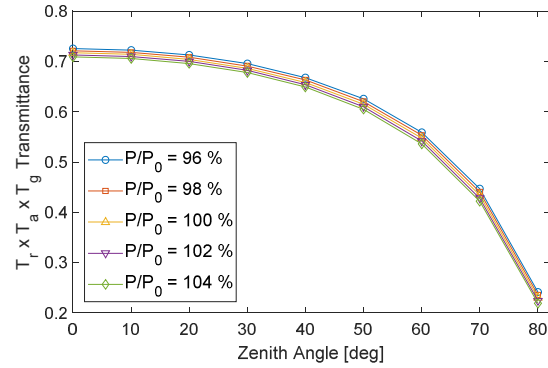


Fig. 3 Combined transmittance of Rayleigh, aerosol, and gas versus zenith angle over five relative air pressures.

Second, the ϵ_w is calculated from the dew point (DP) [8]. The equation is given as follows:

$$\epsilon_w = 0.1 \times e^{(2.2572 + 0.05454 \times DP)} \text{ (cm)}. \quad (5)$$

The DP is calculated from the temperature (T) and the relative humidity (RH) in the weather forecast data [9]. The equation is given as follows:

$$DP = \frac{243.04 \times \left(\ln \left(\frac{RH}{100} \right) + \frac{17.625 \times T}{243.04 + T} \right)}{17.625 - \left(\ln \left(\frac{RH}{100} \right) + \frac{17.625 \times T}{243.04 + T} \right)}. \quad (6)$$

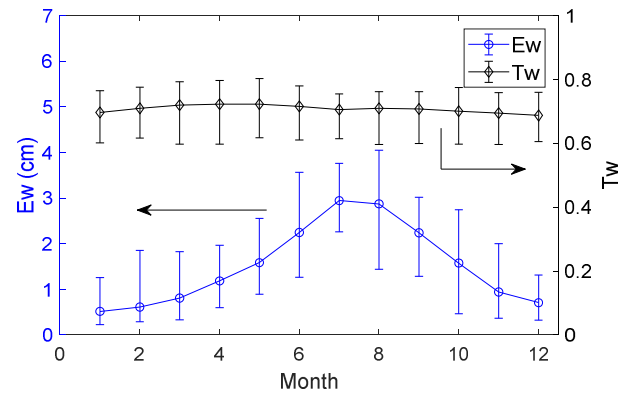


Fig. 4 Monthly precipitable water-vapor thickness (ϵ_w) and water-vapor transmittance (T_w).

How much does the PWVT, ϵ_w , affect the air transmittance? Fig. 4 shows the monthly average and deviation of the PWVT, ϵ_w , and the WVT, T_w , based on a certain weather data of one year. The monthly variation of ϵ_w is large compared to the

average value; it causes the deviation of T_w . As in Fig. 4, T_w has monthly average transmittance errors of $-0.1 \sim 0.066$. Those transmittance errors will cause hourly solar radiation prediction error. Therefore, the use of the hourly ε_w calculated from temperature and relative humidity, not a monthly average value, is recommended to reduce the radiation prediction error.

As a result, monthly average air pressures do not cause a large prediction error and can be used to replace hourly air pressure. On the other hand, PWVT causes variation of transmittance; and monthly average PWVT is not a good choice for precise prediction. Hourly PWVT calculated from weather forecast data such temperature and humidity is a better choice.

III. SIMULATION AND ANALYSIS

The measured hourly data for validation were obtained from the Korea Meteorological Administration (KMA) located at Seoul (longitude = 126.966° , latitude = 37.571°) during 2016. The obtained weather data includes GHI, temperature, humidity, and CCI. The CCI ranges from 0 to 10. The unit of the GHI is converted from $\text{MJ/m}^2/\text{h}$ to W/m^2 . Before validating the proposed prediction model, preprocessing was executed on the obtained weather data by excluding data that have no GHI, CCI, temperature, or relative humidity. The zero values of GHI are also excluded. After the preprocessing, 4,391 data points remained and were used for generation of solar radiation of the proposed prediction model. The regional atmospheric data in Seoul are also used.

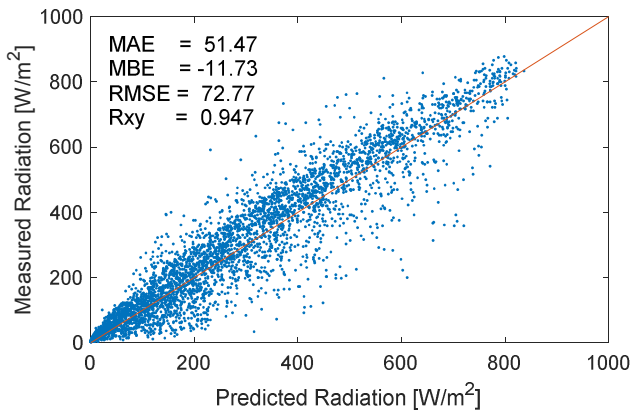


Fig. 5. Correlation between predicted and measured GHIs during one year.

Fig. 5 shows the correlation between predicted and measured GHI values during one year. The diagonal line means exactly the same radiation. The mean absolute error (MAE), mean bias error (MBE), root mean square error (RMSE), and cross correlation coefficient (R_{xy}) are 51.47 W/m^2 , -11.73 W/m^2 , 72.77 W/m^2 , and 0.947 , respectively. The negative MBE means that the proposed prediction model

slightly underestimates solar radiation of the year. The distributed dots are more sparsely scattered under the diagonal line than over the diagonal line. The high cross correlation coefficient of 0.947 shows the validity of the proposed prediction model. The dots distributed near the diagonal line describe a good cross correlation between the predicted and measured radiations.

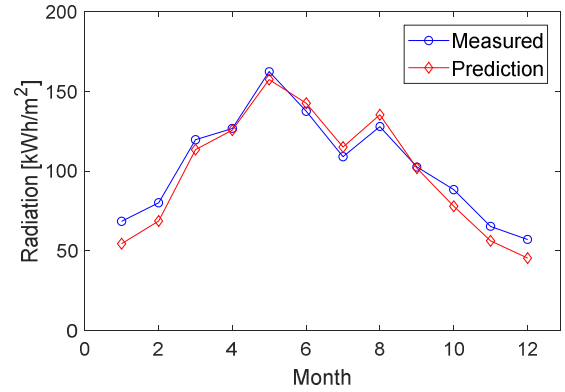


Fig. 6. Monthly total solar radiation on the unit area (m^2) in case of predicted and measured radiation.

Solar radiation prediction depends on the weather forecast. The effects of weather data on prediction may slightly differ depending on seasonal conditions. Fig. 6 shows the monthly total solar radiations, the sum of the whole radiation of a month. The solar radiation unit is converted from W/m^2 to kWh/m^2 . The predicted radiation well matches the measured radiation. In winter, the predicted radiation is slightly less than the measured one. Underestimation in winter explains the negative MBE in Fig. 5.

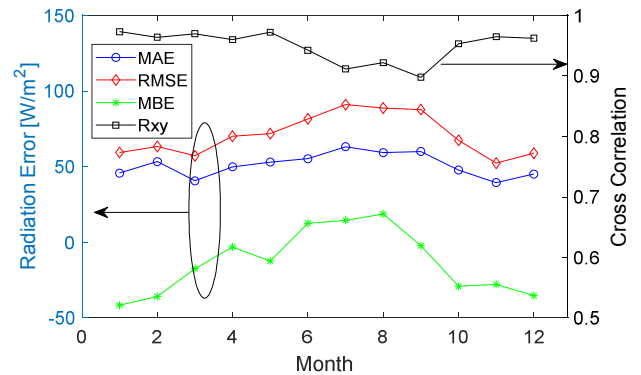


Fig. 7. Monthly calculated values of MAE, RMSE, MBE, and R_{xy} .

Fig. 7 shows the monthly calculated values of MAE, RMSE, MBE, and R_{xy} . The MBE is negative in winter and positive in summer; the negative MBE is larger than the positive one. As a result, the MBE is negative as in Fig. 5. The proposed model underestimates GHIs in winter and slightly overestimates them

in summer. The MAE and RMSE are larger in summer than in winter. It attributes to a relatively large radiation in summer due to the high altitude of the sun. The R_{xy} ranges from 0.897 ~ 0.973. Those of July, August, and September are slightly lower than other months. It may attribute to large weather change in those months. The predicted and measured radiations are highly correlated with one another; it shows the validity of the proposed prediction model.

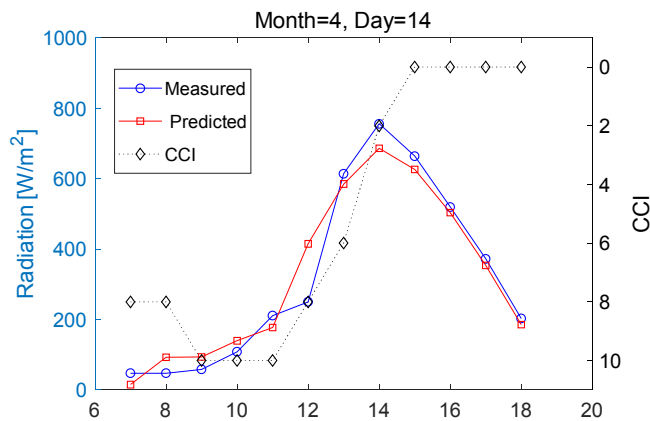


Fig. 8. Hourly predicted and measured radiations versus cloud cover index during one day (April 4).

The solar altitude and CCI mainly affect the solar radiation. The higher the solar altitude is, the larger the solar radiation is. Contrarily, the more cloudy it is, the less the solar radiation is. Fig. 8 shows hourly radiation distribution during one day. In the morning, it is cloudy; in the afternoon, it is becoming clear. A variable cloudy day, April 14, is selected to show the prediction performance. The CCI 0 and 10 mean a clear and the cloudiest sky, respectively. In the morning, the cloudy sky reduces the solar radiation on the surface. From twelve o'clock, the sky is becoming clear. Then, the solar radiation pattern follows a clear sky one. Fig. 8 shows both cloudy and clear day's measurement and prediction. The predicted radiations sometimes slightly deviate from the measured ones under the cloudy sky in the morning. Despite the slight deviation, the proposed prediction model well estimates hourly solar radiation. The simulation results validate the proposed solar radiation prediction model.

VI. CONCLUSION

This paper proposed a solar radiation prediction model using weather forecast data and regional atmospheric data. It showed that the air pressure variation negligibly affects radiation; and monthly average air pressures from the past weather data can replace air pressures excluded from the weather forecast. It also showed that the PWVT, ε_w , affects the water-vapor transmittance and needs to be calculated from the

temperature and humidity included in the weather forecast data. The proposed solar radiation prediction model was validated through simulations based on the obtained weather data during one year of 2016 in Seoul, Republic of Korea. The cross correlation between the predicted and measured radiations for one year is high with 0.947. The MAE and RMSE are 51.47 W/m² and 72.77 W/m². The MBE is - 11.73 W/m². The negative MBE shows that the proposed model underestimates solar radiation. Underestimation occurs mainly in winter. In a clear sky, the predicted radiations well match the measured ones; on the other hand, in a cloudy sky, the prediction is difficulty and deviates from the measured one. Overall, the simulation results validate the proposed solar radiation prediction model. The proposed prediction model using both weather forecast data and regional atmospheric data is expected to contribute to precise prediction of hourly solar radiation; and the precise prediction will enhance an efficient use of solar energy, that is, photovoltaic generation.

ACKNOWLEDGEMENT

This work was supported by the Korea Institute of Energy Technology Evaluation and Planning (KETEP) and the Ministry of Trade, Industry & Energy (MOTIE) of the Republic of Korea (No. 20172410100040).

REFERENCES

- [1] H. D. Kambezidis, B. E. Psilooglou, D. Karagiannis, U. C. Dumka, and D. G. Kaskaoutis, "Recent improvements of the meteorological radiation model for solar irradiance estimates under all-sky conditions," *Renewable Energy*, vol. 93, pp. 142-158, 2016.
- [2] T. Muneer and S. Younes, "The all-sky meteorological radiation model: proposed improvements," *Applied Energy*, vol. 83, pp. 436-450, 2006.
- [3] S. -W. Park, S. Y. Son, J. -B. Park, K. Y. Lee, and H. Hwang, "An irradiation prediction model for photovoltaic power generation under limited weather information," in *19th IFAC World Congress*, 2014, p.3670-3675.
- [4] L. T. Wong and W. K. Chow, "Solar radiation model," *Applied Energy*, vol. 69, pp. 191-224, 2001.
- [5] R. Bird and C. Riordan, "Simple solar spectral model for direct and diffuse irradiance on horizontal and tilted planes at the earth's surface for cloudless atmospheres," *Journal of Climate and Applied Meteorology*, vol. 25, pp. 87-97, 1986.
- [6] M. A. Machler, "Parameterization of solar irradiation under clear skies," *PhD Thesis*, University of British Columbia, 1983.
- [7] T. Muneer and M. S. Gul, "Evaluation of sunshine and cloud cover based models for generating solar radiation data," *Energy Conversion & Management*, vol. 41, pp. 461-482, 2000.
- [8] O. Behar, A. Khellaf, and K. Mohammadi, "Comparison of solar radiation models and their validation under Algerian climate - The case of direct irradiance," *Energy Conversion and Management*, vol. 98, pp. 236-251, 2015.
- [9] M. G. Lawrence, "The relationship between relative humidity and the dewpoint temperature in moist air," *Bulletin of the American Meteorological Society*, vol. 86, pp. 225-233, 2005.